Atomistic modeling of carbon Cottrell atmospheres in bcc iron

2013 J. Phys.: Condens. Matter 25 025401

(http://iopscience.iop.org/0953-8984/25/2/025401)

J. Phys.: Condens. Matter **25** (2013) 025401 (7pp) doi:10.1088/0953-8984/25/2/025401

Atomistic modeling of carbon Cottrell atmospheres in bcc iron

R G A Veiga[1,2], M Perez[2], C S Becquart[3,4] and C Domain[4,5]

[1] Escola Politécnica/Departamento de Engenharia Metalúrgica e de Materiais, Universidade de São Paulo, Avenida Prof. Mello de Morais, no. 2463, Butantã, CEP 05508-030, São Paulo, SP, Brazil
[2] Université de Lyon, INSA Lyon, Laboratoire MATEIS, UMR CNRS 5510, 25 Avenue Jean Capelle, F69621, Villeurbanne, France
[3] Unité Matériaux et Transformations (UMET), Ecole Nationale Supérieure de Chimie de Lille, UMR CNRS 8207, Bâtiment C6, F-59655 Villeneuve d'Ascq Cedex, France
[4] Laboratoire commun EDF-CNRS Etude et Modélisation des Microstructures pour le Vieillissement des Matériaux (EM2VM), France
[5] EDF, Recherche et Développement, Matériaux et Mécanique des Composants, Les Renardières, F-77250 Moret sur Loing, France

E-mail: rgaveiga@usp.br

Received 29 August 2012, in final form 29 October 2012
Published 26 November 2012
Online at stacks.iop.org/JPhysCM/25/025401

Abstract
Atomistic simulations with an EAM interatomic potential were used to evaluate carbon–dislocation binding energies in bcc iron. These binding energies were then used to calculate the occupation probability of interstitial sites in the vicinity of an edge and a screw dislocation. The saturation concentration due to carbon–carbon interactions was also estimated by atomistic simulations in the dislocation core and taken as an upper limit for carbon concentration in a Cottrell atmosphere. We obtained a maximum concentration of 10 ± 1 at.% C at $T = 0$ K within a radius of 1 nm from the dislocation lines. The spatial carbon distributions around the line defects revealed that the Cottrell atmosphere associated with an edge dislocation is denser than that around a screw dislocation, in contrast with the predictions of the classical model of Cochardt and colleagues. Moreover, the present Cottrell atmosphere model is in reasonable quantitative accord with the three-dimensional atom probe data available in the literature.

(Some figures may appear in colour only in the online journal)

1. Introduction

Dislocations are linear defects commonly found in crystalline materials that have undergone plastic deformation. Indeed, dislocation mobility is supposed to play a major role in plasticity [1], particularly in metals. In the late 1940s, Cottrell and Bilby proposed that steel hardening observed during strain aging experiments could be understood in terms of dislocation pinning by impurities that migrate to the vicinity of the line defects [2]. As a consequence of continuous segregation, clouds of impurities, since then known as Cottrell atmospheres, were predicted to form in the surroundings of dislocations. Following the theoretical insight of Cottrell and Bilby, some classical works based on the elasticity theory investigated the interaction of carbon atoms with dislocations in bcc iron, which was expected to be the driving force that would lead to the formation of Cottrell atmospheres [3–5]. Of special importance was to determine the maximum number of carbon atoms that a single dislocation could bind in its atmosphere. Cochardt and co-workers proposed that the saturation concentration is achieved when an additional carbon atom in a certain volume near the dislocation is no longer able to reduce the elastic energy of the crystal [5]. In other words, removing a carbon atom in solid solution from the iron matrix, where it does not interact with the dislocation, to bring it to the dislocation vicinity, results in a less stable configuration. In that work, a crude estimate was presented in which a dislocation can bind up to 15 carbon atoms per

atomic plane at room temperature. The extent of a Cottrell atmosphere as a function of temperature was also estimated by the same authors, assuming that a carbon atom, to be part of the atmosphere, should occupy an interstitial site for which its binding energy to the dislocation is larger than the thermal energy $k_B T$. At $T = 300$ K, a Cottrell atmosphere should extend up to 7.5 nm away from the dislocation line.

On the experimental front, the segregation of solute atoms to dislocations is one of the most difficult microstructural features to characterize, owing to the small extent of Cottrell atmospheres. Despite the difficulties, and even if not routinely, three-dimensional atom probe (3DAP) techniques have allowed us to successfully image Cottrell atmospheres [6–9]. Chang demonstrated carbon segregation to dislocations in low carbon lath martensites by superimposing field ion micrographs and gated carbon images taken in the imaging atom probe [6], providing the first direct observation of a carbon Cottrell atmosphere in iron more than three decades after the pioneering work of Cottrell and Bilby. However, due to the limitations of the experimental apparatus, Chang's work was not fully quantitative insofar as not all carbon atoms were detected.

Wilde and co-workers later extended Chang's work and mapped a three-dimensional distribution of carbon atoms around a dislocation in low carbon martensite with an energy-compensated optical position sensitive atom probe (ECOPoSAP) in conjunction with field ion microscopy (FIM) [8]. Solute enhancement in the vicinity of the line defect was clearly demonstrated: the carbon atoms formed a disperse cloud extending about 7 nm outwards from the dislocation core, with about 105 carbon atoms per 10^{-9} m of dislocation. The shape of the solute enhanced region, showing three lobes separated by approximately 120°, led the authors of [8] to conclude that it was likely to be a screw dislocation. However, as Wilde and co-workers recognized, it is not a trivial task to characterize the dislocation type in FIM, and, as has been pointed out by Miller [9], except in a few special cases where the closure failure of the Burgers circuit is visible in the atom maps (for instance, in [7]), it is not normally possible to distinguish the dislocation type or the precise location of the dislocation line from the atom probe data. Moreover, even in these special cases, the applied electric field imposes a mechanical stress on the specimen that may alter the precise relationship of the dislocation to the atmosphere.

This paper goes beyond the classical works based on the elasticity theory in the sense that atomic-level information is fully taken into account in the surroundings of the line defects. Moreover, from the data of atomistic simulations, we estimated the saturation concentration in the core of an edge and a screw dislocation in α-iron considering not only carbon–dislocation interactions but also carbon–carbon interactions. The spatial distribution of carbon atoms in a Cottrell atmosphere model is also compared to the atom probe data for the Fe–C system available in the literature [8].

2. Modeling approach

2.1. Statistical physics

The problem of finding the average concentration of solute atoms in a Cottrell atmosphere under the condition of thermodynamic equilibrium has been addressed since such atmospheres were first proposed as an explanation of the static strain aging phenomenon [2]. For this purpose, Cottrell and Bilby employed the Maxwell–Boltzmann formula around an edge dislocation:

$$\frac{n_i}{n_0} = \exp\left(\frac{E_i^{\mathrm{b}}}{k_B T}\right). \tag{1}$$

In equation (1), n_i is the number of solute atoms occupying sites with solute–dislocation binding energy E_i^{b} and n_0 is the background (matrix) solute concentration. Cottrell and Bilby verified that this distribution holds for dilute carbon concentrations in the far-field, where E_i^{b} is small. However, it fails near the dislocation core (when the separation between the solute and the dislocation falls below 1 nm), where E_i^{b} assumes the largest values. In this region and at room temperature, Maxwell–Boltzmann statistics yields impossibly large values of the ratio n_i/n_0 (of the order of 10^{11}), which implies that many carbon atoms might be found occupying the same interstitial site.

In an attempt to provide a more reasonable distribution taking into account the saturation of interstitial sites, Louat proposed the following equation [3]:

$$\frac{n_i}{n_0} = \frac{N_i - n_i}{N_0 - n_0} \exp\left(\frac{E_i^{\mathrm{b}} - E_0^{\mathrm{b}}}{k_B T}\right) \tag{2}$$

where N_0 and n_0 are the total number of sites and number of occupied sites, respectively, of a reference state of energy E_0^{b}. Louat's derivation was based on the following assumptions:

(1) the region near a dislocation may be divided into a number of discrete sub-regions characterized by a unique solute–dislocation binding energy (e.g. the octahedral sites in α-Fe that can be occupied by interstitial carbon atoms);
(2) each sub-region can be occupied by only one solute atom at a time;
(3) the interaction between solute atoms in the atmosphere may be neglected.

An important remark made by Beshers is that these assumptions are the same as the ones on which Fermi–Dirac statistics are based, that is, the problem here also boils down to how to distribute indistinguishable particles with negligible mutual interaction in discrete states with a maximum occupancy of one particle per state [4].

Equation (2) can be readily rearranged as follows:

$$\frac{n_i}{N_i - n_i} = \frac{n_0}{N_0 - n_0} \exp\left(\frac{E_i^{\mathrm{b}} - E_0^{\mathrm{b}}}{k_B T}\right). \tag{3}$$

If we take as the reference state an octahedral site at a large distance from the dislocation line, where the interaction between the defects vanishes, $E_0^{\mathrm{b}} \to 0$ and can be eliminated from equation (3). Moreover, there is a large degeneracy in energy: the total number of sites with a given energy is as great as the number of these sites per dislocation unit length

multiplied by the total dislocation length. It is thus more convenient if we express equation (3) in terms of the fractional occupancies $\bar{n}_i = n_i/N_i$ and $\bar{n}_0 = n_0/N_0$:

$$\frac{\bar{n}_i}{1-\bar{n}_i} = \frac{\bar{n}_0}{1-\bar{n}_0} \exp\left(\frac{E_i^{\mathrm{b}}}{k_{\mathrm{B}}T}\right) \tag{4}$$

where $\bar{n}_i$ is the fractional occupancy of a site located in the neighborhood of a dislocation characterized by the binding energy E_i^{b}. Provided that the dislocation density is very low, the defective region surrounding the line defect is much smaller than the non-strained matrix. This implies $\{N_i\} \ll N_0$, thus carbon concentration in the matrix (taken as a reservoir of carbon atoms) remains almost unchanged even after segregation completion and thus the reference fractional occupancy $\bar{n}_0$ remains almost constant.

Before applying equation (4) to model carbon distribution in a Cottrell atmosphere, the carbon–dislocation binding energies in the vicinity of a line defect have to be obtained. This has been accomplished by performing molecular statics simulations.

2.2. Molecular statics

2.2.1. Simulation setup. Molecular statics simulations were performed by LAMMPS [10] with a recently developed Fe–C potential [11] built according to the embedded atom method (EAM) [12], taking into account the modifications in the Fe–C pairwise function described in [13]. In this method, the total energy of an assembly of atoms is obtained by the following equation:

$$E^{\mathrm{tot}} = \tfrac{1}{2}\sum_{i,j}\phi(r_{ij}) + \sum_i F_i\left(\sum_{i\neq j}\rho(r_{ij})\right). \tag{5}$$

Here $\phi(r_{ij})$ is the pairwise interaction between atoms i and j separated by r_{ij}, F_i is the embedding energy of atom i, and $\rho(r_{ij})$ is the electron density induced by atom j at the location of atom i.

The simulation boxes employed in this study consisted of cylinders of radius 15 nm and height 4 nm with an edge or a screw dislocation as the cylinder axis. The iron atoms (about 200 000) have been arranged on a bcc lattice with $a_0 = 0.286$ nm, where a_0 is the equilibrium lattice parameter and its value is given by the EAM potential. The dislocations have been introduced in the simulation boxes by displacing the iron atoms according to the anisotropic elasticity theory of straight line defects [14–16] as implemented in the Babel code [17]. Such a displacement corresponds to the Volterra elastic field created by the dislocation. In both cases, the Burgers vector is $\vec{b} = a_0/2[111]$. These dislocations are the most commonly observed in α-iron. For the edge dislocation, the dislocation line is oriented along the $[1\bar{2}1]$ direction, whereas the dislocation line for the screw dislocation is oriented along the [111] direction. The glide plane of the edge dislocation is a $\{\bar{1}01\}$ plane that divides the simulation box into two halves, one where the crystal is under compression and the other where the crystal is under tension.

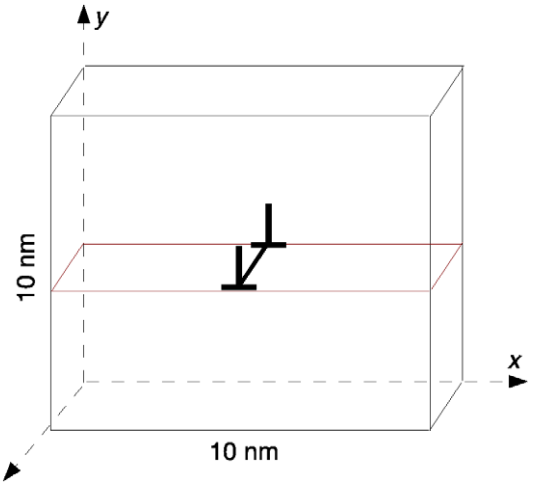

Figure 1. Parallelepipedal region surrounding a dislocation segment where octahedral sites were mapped.

A dislocation is known to destroy the lattice periodicity in directions perpendicular to its line. Consequently, periodic boundary conditions have not been applied in any direction except along the dislocation line. A 2 nm thick (about four times the potential cutoff) outer shell of iron atoms was kept fixed in the simulations. The aim of this rigid boundary condition was to avoid spurious relaxation that might come from free surface effects, so that the true dislocation strain field was permanently reproduced in the far-field.

2.2.2. Carbon–dislocation interactions: binding energies. For both dislocation types, all interstitial positions corresponding to octahedral (O) sites within a parallelepiped of volume $10 \times 10 \times \hat{z}$ nm^3, where $\hat{z} = a_0\sqrt{6} \approx 0.7$ nm (edge) or $\hat{z} = a_0\sqrt{3} \approx 0.5$ nm (screw), were mapped (see figure 1). In bcc iron, an octahedral site is found at the midpoint between every two neighboring iron atoms situated at the corners of the cubic cell (see figure 2). There are three O variants according to the direction of the Fe–Fe pair: [100], [010], and [001]. For every mapped interstitial position, a molecular statics simulation was launched with a single carbon atom at that position, and full energy minimization was carried out up to the point where the interatomic forces were less than 10^{-2} eV nm^{-1}.

The strength and type of the interaction (attractive or repulsive) between a carbon atom and a dislocation as a function of the relative positions of the defects is given by the corresponding binding energy, defined as follows:

$$E^{\mathrm{b}} = E_{\mathrm{C}} + E_{\mathrm{dislo}} - E_{\mathrm{C+dislo}}. \tag{6}$$

In equation (6), E_{C} is the energy added by an isolated carbon atom occupying an O site in the iron matrix after relaxation, E_{dislo} is the total potential energy of the simulation box containing the dislocation, and $E_{\mathrm{C+dislo}}$ refers to the total potential energy of the same simulation box with a single carbon atom in an O site. $E^{\mathrm{b}} > 0$ indicates an attractive interaction between the point and the line defect, whereas $E^{\mathrm{b}} < 0$ means that the dislocation repels the carbon atom.

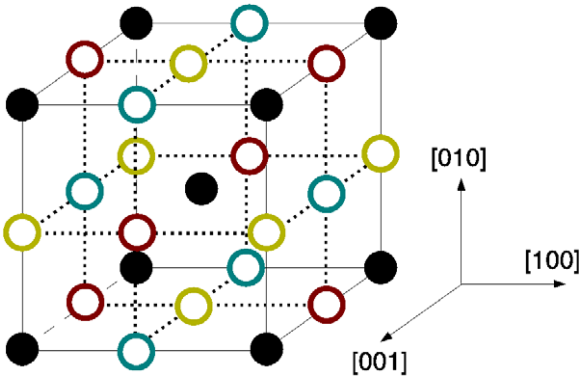

Figure 2. A schematic illustration of the positions of the three different O sites (variants) in the bcc unit cell (open circles). The iron atoms are represented by filled black circles.

2.2.3. Carbon–carbon interactions: saturation concentration. Louat's formulation provides better results than Maxwell–Boltzmann statistics, but it still fails in the vicinity of the dislocation core. As pointed out by Beshers [4], in this region, where the largest carbon–dislocation binding energies are found, the occupation probability $\bar{n}_i$ given by equation (4) is larger than 99% at room temperature. This corresponds to about three carbon atoms per iron atom within a distance of b from the dislocation line, a carbon concentration much higher than the highest concentration experimentally observed. One can readily deduce that the reason behind this result is that the third assumption on which Louat based the derivation of equation (2) is not valid when the atmosphere becomes too dense. Indeed, depending on their relative positions in the iron matrix, two neighboring carbon atoms can attract or repel each other with binding energies of up to 1.50 eV or −1.67 eV, respectively, according to density functional theory (DFT) calculations [11]. Therefore, the saturation effects due to carbon–carbon interactions also have to be addressed somehow before building up a carbon Cottrell atmosphere model.

In the present work, the saturation concentration was determined from carbon distributions in the core of an edge or a screw dislocation that corresponded to energy minima of the Fe–C system. We considered that an energy minimum (carbon-saturated) configuration was achieved when there was no single change in the system state (i.e. insertion or removal of a carbon atom) able to reduce the system energy. In other words, the Fe–C system would have to visit one or more configurations with higher energies to leave the current configuration. The reference state was a configuration where no carbon atom is found in the dislocation core. The dislocation core, in turn, was defined as a cylinder of radius $4b \approx 1$ nm surrounding the dislocation line. In this volume the interaction between a single carbon atom and a dislocation is strongest—up to 0.65 eV (carbon–edge dislocation interaction) and 0.41 eV (carbon–screw dislocation interaction) according to the EAM Fe–C potential—and thus it is the region where we should expect to find the sites with the highest occupancy probabilities $\{\bar{n}_i\}$. In order to obtain an energy minimum of the Fe–C system, a script implementing an iterative energy minimization algorithm was employed. Taking the reference state as the initial state, at every script iteration a carbon atom was either inserted in or removed from an interstitial site chosen at random and then the total energy of the newly generated configuration was obtained by molecular statics simulations as usual[6]. The formation energy of the ith configuration was calculated as follows:

$$E_i^{\mathrm{f}} = mE_{\mathrm{C}} + E_{\mathrm{dislo}} - E_{m\mathrm{C+dislo}} \tag{7}$$

where E_{C} and E_{dislo} have the same meaning as in equation (6); $E_{m\mathrm{C+dislo}}$ is the total energy of the simulation box with either an edge or a screw dislocation and m carbon atoms[7] distributed in the dislocation core in a particular manner. At the end of an iteration, the ith configuration was accepted only if it lowered the energy of the Fe–C system compared to the previously accepted configuration (i.e. if $E_i^{\mathrm{f}} > E_{\mathrm{acc}}^{\mathrm{f}}$); otherwise, it was rejected and the previously accepted configuration was kept for the next iteration. The script stopped after a number of configurations were rejected (in this work, 1000).

3. Results and discussion

3.1. Spatial carbon distribution in a Cottrell atmosphere

A number of random carbon-saturated configurations was generated by the iterative minimization script briefly described in section 2. We noticed that carbon spatial distribution is more uniform inside the core of a screw dislocation, whereas around an edge dislocation most of the carbon atoms (more than 90%) are found above the glide plane. Very low carbon concentration is actually expected below the glide plane where the compressive stress predominates and the interstitial volumes for accommodating carbon atoms are smallest.

At a first sight, one can infer that the region defined as the core of a screw dislocation is able to absorb about twice as many carbon atoms as the core of an edge dislocation, as was in fact suggested by Cochardt and co-workers [5]. What is observed in the atomistic data is that the tensile half of the core region of an edge dislocation can accommodate almost as many carbon atoms as the entire core of a screw dislocation. A reasonable explanation is that the carbon–carbon repulsion in this volume, which is half the volume where the carbon atoms are arranged around a screw dislocation, is compensated by the carbon–dislocation attractive interactions, known to be much stronger for an edge dislocation. Indeed, the mean

[6] Dilatation/contraction of the simulation box due to carbon insertion/removal has not been taken into account. The pressure consequently varied inside the simulation box, which certainly was a source of errors, but a compromise between the accuracy in the simulation results and required CPU time could not be put aside considering the large number of configurations that had to be tested in order to achieve the energy minima.

[7] The Fe–C EAM potential used in this work has been developed to address dilute carbon concentrations in bcc iron. However, as one can see in [11, 21], this potential also performed reasonably well, compared to *ab initio* calculations, for systems where two or more carbon atoms are expected to interact with each other.

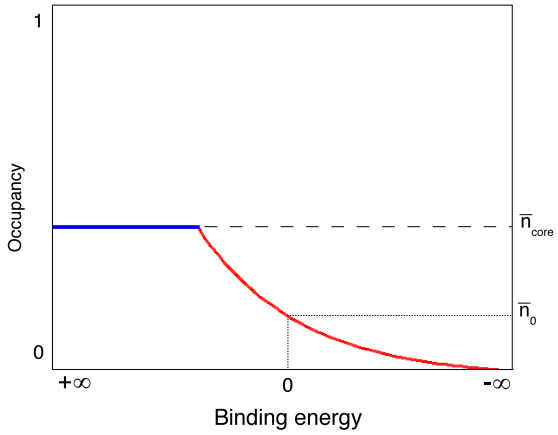

Figure 3. The occupancy of interstitial sites in the volume of interest is assumed to be a function of carbon–dislocation binding energies and is given by equation (4). In principle, it can vary from 0 to 1; in this work, however, we took the mean occupancy in the core $\bar{n}_{core}$ when the saturation condition is achieved at $T = 0$ K as an upper limit in order to avoid unphysically high carbon concentrations.

formation energy $\langle E^f \rangle$ of the saturated carbon distributions is 6.5 ± 0.5 eV per 10^{-9} m of dislocation (about 0.20 eV per carbon atom) in the core of an edge dislocation and 5.5 ± 0.5 eV per 10^{-9} m of dislocation (about 0.17 eV per carbon atom) in the core of a screw dislocation. The simulations revealed that the saturated concentrations corresponded to 10 ± 1 at.% C in the dislocation cores at $T = 0$ K. This is equivalent to 31 ± 2 carbon atoms per 10^{-9} m of dislocation within a radius of $4b$ from the dislocation line. For the sake of comparison, the experimental results from atom probe data provided by Wilde [8] and Miller [18] presented a maximum carbon concentration of 6–8 at.% C in the neighborhood of dislocations in iron–carbon martensite at room temperature.

The mean fractional occupancy in the dislocation core $\bar{n}_{core}$, taken as the ratio $\langle n_{occ} \rangle / N_{sites}$ (where $\langle n_{occ} \rangle$ is the final number of occupied sites on average and N_{sites} is the total number of interstitial sites), was only 0.06 and 0.04 in the tensile half of the core of an edge dislocation and in the core of a screw dislocation, respectively. Therefore, the average occupation probability of interstitial sites in the core of dislocations is much lower than unity. Henceforth we assumed that the saturation concentration in the dislocation core at $T = 0$ K represented an upper limit for carbon concentration in the Cottrell atmosphere to be modeled by equation (4). This is to say that, irrespective of the temperature and carbon concentration in the reservoir, the occupancy of an interstitial site could not be larger than $\bar{n}_{core}$, as schematically shown in figure 3.

Equation (4) with the binding energies obtained from molecular statics simulations, considering the saturation concentration limit defined in the paragraph above, was used to calculate the fractional occupancies around an edge and a screw dislocation at room temperature ($T = 300$ K). Owing to the large difference in the stress field around an edge and a screw dislocation, one should expect the atoms in a Cottrell atmosphere to be arranged differently depending on the dislocation type. On the other hand, although the carbon concentration near the line defects should vary depending on either the aging temperature or carbon content, it seems to be a reasonable assumption that these variables have a minor effect on the shape of the Cottrell atmosphere. Figure 4 shows the spatial distribution of the fractional occupancies $\{\bar{n}_i\}$ around both dislocation types at $T = 300$ K. We used a value of $\bar{n}_0$ corresponding to a background carbon concentration of 0.33 at.% C. As expected, the $\{\bar{n}_i\}$ are much larger above the glide plane of the edge dislocation, where the crystal is under tension, than below, where it is under compression. Around a screw dislocation, in turn, carbon enhancement is more likely to be observed in three lobe-shaped regions separated by 120°, as predicted by earlier theoretical work [5] and apparently observed in the 3D images of a Cottrell atmosphere by the authors of [8].

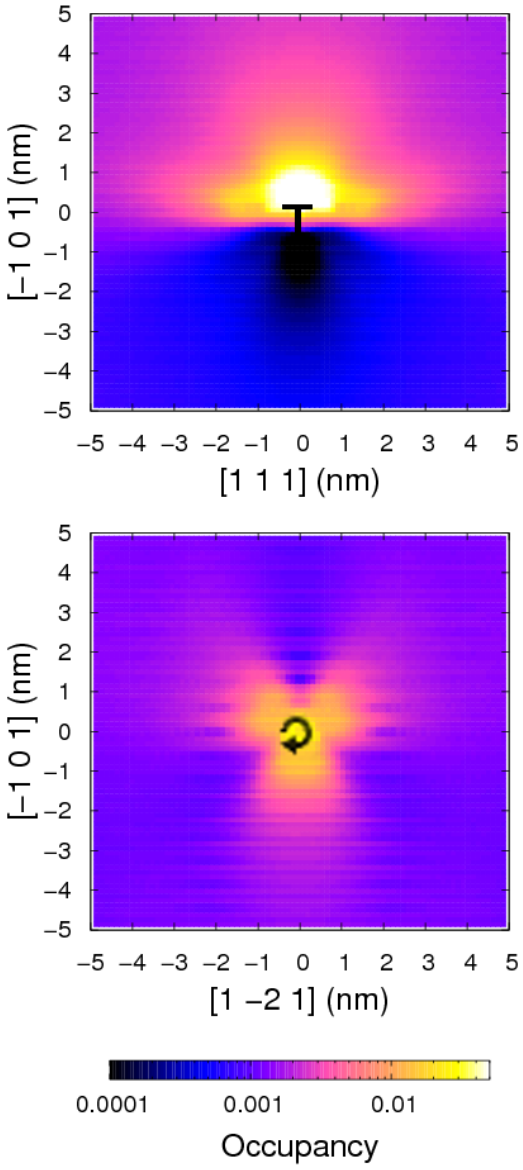

Figure 4. Fractional occupancy distribution in the vicinity of an edge (top) and a screw (bottom) dislocation at $T = 300$ K (plot area: 10×10 nm^2). A background concentration of 0.33 at.% C was assumed.

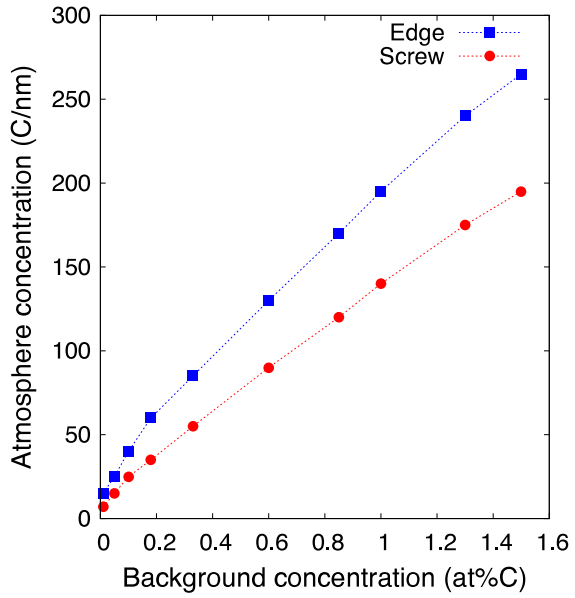

Figure 5. Number of carbon atoms per unit length of dislocation (in nm^{-1}) at $T = 300$ K as a function of the background carbon concentration (volume: $10 \times 10 \times 1$ nm^3).

Once knowing the fractional occupancies of the interstitial sites in the volume of interest, the number of carbon atoms per unit length of dislocation corresponding to background carbon concentrations in the 0.01–1.5 at.% C range was estimated and is presented in figure 5. As one can see, the Cottrell atmospheres that form predominantly in the tensile half of edge dislocations are significantly denser than the carbon clouds around screw dislocations. This is particularly true under the condition of low carbon content, in which the relative difference can be larger than 100%.

Although the spatial distribution of fractional occupancies in figure 4 may induce the conclusion that the dislocation type could be characterized unambiguously in experimental images by the shape of the corresponding Cottrell atmosphere, such atmospheres are more likely to be viewed as disperse clouds of carbon atoms. This feature was experimentally observed by the authors of [8] and it can also be seen in figure 6, where the occupied sites around an edge and a screw dislocation were randomly determined in three different $10 \times 10 \times 1$ nm^3 volumes (per dislocation type) using the corresponding occupancy probabilities, assuming again a background carbon concentration of 0.33 at.% C at $T = 300$ K.

3.2. Comparison to atom probe data

The theoretical treatment of carbon Cottrell atmospheres presented in this work is essentially qualitative, although we have pursued a quantitative description too. Some considerations have to be made before comparing our theoretical predictions to the experimental data available in the literature. First, many features of experimental samples are too complex to be taken into account by atomic-level models that have to be kept as simple as possible to be tractable. For instance, a realistic sample may contain a high dislocation density (with dislocations in a variety of orientations, forming loops or junctions, and so on), as well as other defects that can act as sinks for impurities (e.g., grain and lath boundaries and precipitate carbides).

Table 1. Number of carbon atoms per unit length of dislocation, in nm^{-1}, in the zone defined in figure 1 (background concentration: 0.85 at.% C).

Method	References	Dislocation type	$N_{C/l}$ (nm^{-1})
Atom probe	[8]	Screw	105
Theoretical distribution	This work	Edge	170
	This work	Screw	120

Second, there is no indisputable criterion to define the extent of a Cottrell atmosphere. On the theoretical side, it was proposed by Cochardt and co-workers and since then accepted that a Cottrell atmosphere should extend up to the limit in which the carbon–dislocation binding energy beats the thermal energy $k_B T$ [5]. However, to our knowledge, it is not possible to obtain those binding energies by any experimental method, thus Cochardt's criterion cannot be applied to experimental data. Instead, Cottrell atmospheres in the atom probe data reported by [8, 9, 19] were visually identified as impurity enriched zones (in comparison to the surrounding matrix). Such an approach means that the extent of the imaged atmospheres is somewhat human biased and can vary significantly from one experiment to another.

In contrast with a recent work on carbon–dislocation interactions that used Cochardt's criterion to estimate the extent of Cottrell atmospheres [20], we have considered in this study only the portion of the atmosphere contained inside the fixed volume parallelepipedal region depicted in figure 1, the rectangular cross section of which (10×10 nm^2) corresponds approximately to the width and height of the 'window' of the atom probe experiments shown in [8].

In table 1, where $N_{C/l}$ is the number of carbon atoms per unit of dislocation length, we examine how the model results compare to the atom probe data of Wilde and co-workers [8]. We considered $\bar{n}_0$ corresponding to a matrix concentration of 0.85 at.% C, the same value as the carbon content in the experimental sample. However, it is worth mentioning again that in the model the dislocation surroundings are connected to an infinite carbon reservoir, such that no carbon depletion occurs in the matrix due to segregation, an important difference with respect to what is usually reported in aging experiments.

Wilde and colleagues observed that, during the specimen aging, about 105 carbon atoms per 10^{-9} m of dislocation segregated to form an atmosphere around the imaged line defect. One can see that the experimental value is much closer (a difference of about 15%) to what the present model predicted around a screw dislocation (i.e. about 120 carbon atoms per 10^{-9} m of dislocation). In other words, despite the simplifications of the model, the quantitative agreement with the experimental data still is remarkable. Moreover, it seems that the model also supports the conclusion of the authors of [8] that the dislocation around which the imaged atmosphere formed was a screw.

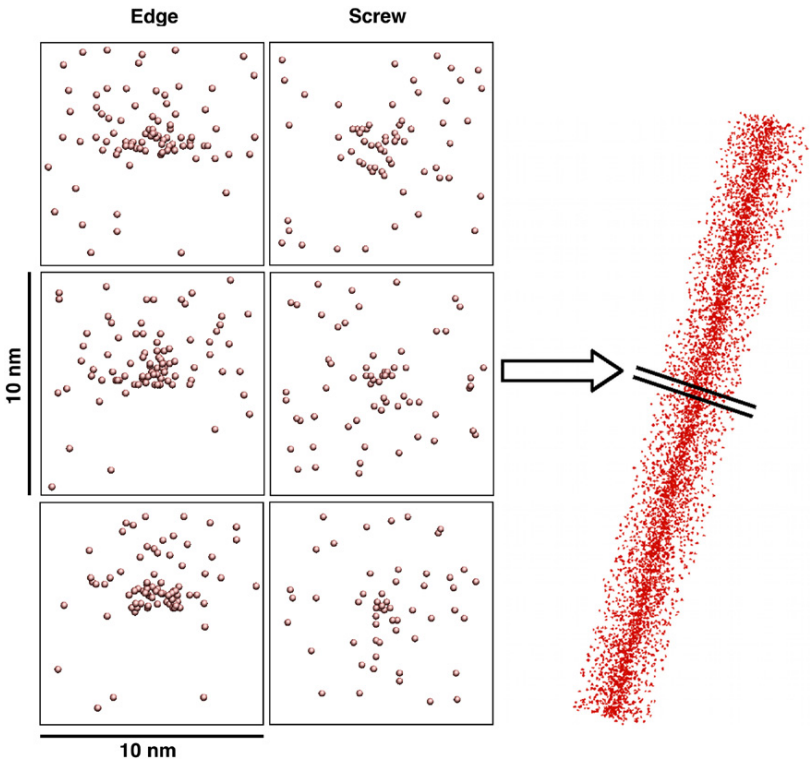

Figure 6. Six 1 nm thick slices out of Cottrell atmospheres generated according to the model around an edge and a screw dislocation (plot area: 10×10 nm^2). The carbon atoms are represented as red balls, whereas the iron atoms are not shown for clarity. A background carbon concentration of 0.33 at.% C was assumed.

4. Conclusions

To summarize, we have presented in this paper an approach that uses the statistical distribution proposed by Louat, which is based on the same assumptions as Fermi–Dirac statistics, combined with the estimate of carbon saturation concentration in the core of dislocations at $T = 0$ K to model the spatial carbon distribution in a Cottrell atmosphere as a function of the carbon concentration in the α-Fe matrix, taken as an infinite reservoir of carbon atoms. The model, though essentially qualitative, was seen to be in reasonable quantitative agreement with experimental data provided by atom probe techniques as reported by [8]. Regarding the maximum carbon concentration, it was estimated to be about 10 at.% C in the core of an edge and a screw dislocation at $T = 0$ K. Additionally, the coordinates of carbon atoms in Cottrell atmospheres generated according to this model can be used as the input of atomistic simulations of dislocation dynamics (e.g. to investigate the effect of Cottrell atmospheres on dislocation glide), which is the logical next step of this work.

Acknowledgments

RGAV gratefully acknowledges EDF (France) and FAPESP Project 2011/19564-6 (Brazil) for funding.

References

[1] Hirth J P and Lothe J 1968 *Theory of Dislocations* (New York: McGraw-Hill)
[2] Cottrell A H and Bilby B A 1949 *Proc. Phys. Soc.* A **62** 49
[3] Louat N 1956 *Proc. Phys. Soc.* B **69** 459
[4] Beshers D N 1958 *Acta Metall.* **6** 521
[5] Cochardt A W, Shoek G and Wiedersich H 1955 *Acta Metall.* **3** 533
[6] Chang L 1985 *PhD Thesis* Oxford University
[7] Blavette D, Cadel E, Fraczkiewicz A and Menand A 1999 *Science* **286** 2317
[8] Wilde J, Cerezo A and Smith G D W 2000 *Scr. Mater.* **43** 39–48
[9] Miller M K 2006 *Microsc. Res. Tech.* **69** 359
[10] Plimpton S J 1995 *J. Comput. Phys.* **117** 1–19
[11] Becquart C S, Raulot J M, Benecteux G, Domain C, Perez M, Garruchet S and Nguyen H 2007 *Comput. Mater. Sci.* **40** 119–29
[12] Daw M S and Baskes M I 1983 *Phys. Rev. Lett.* **50** 1285
[13] Veiga R G A, Perez M, Becquart C S, Clouet E and Domain C 2011 *Acta Mater.* **59** 6963
[14] Eshelby J D, Read W T and Shockley W 1953 *Acta Metall.* **1** 251
[15] Stroh A N 1962 *J. Math. Phys.* **41** 77
[16] Stroh A N 1958 *Phil. Mag.* **3** 625
[17] Clouet E 2011 *Phys. Rev.* B **84** 224111
[18] Sherman D, Cross S, Kim S, Grandjean F, Long G J and Miller M K 2007 *Metall. Mater. Trans.* A **38A** 1698
[19] Miller M K, Kenik E A, Russell K F, Heatherly L, Hoelzer D T and Maziasz P J 2003 *Mater. Sci. Eng.* A **353** 140
[20] Hanlumyuang Y, Gordon P A, Neeraj T and Chrzan D C 2010 *Acta Mater.* **58** 5481–90
[21] Sinclair C W, Perez M, Veiga R G A and Weck A 2010 *Phys. Rev.* B **81** 224204